



Investigating the interplay of the hydrometeorological and seasonal forest vegetation role in regulating the nitrate flushing in a small torrential catchment

K. Lebar ^{a,*}, D. Kastelec ^b, S. Rusjan ^a

^a University of Ljubljana, Faculty of Civil and Geodetic Engineering, Ljubljana, Slovenia

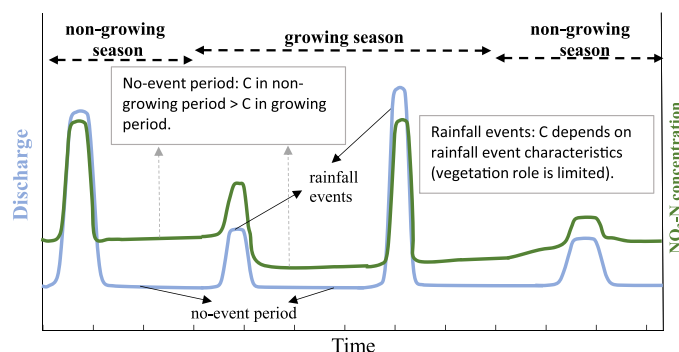
^b University of Ljubljana, Biotechnical Faculty, Ljubljana, Slovenia



HIGHLIGHTS

- Rainfall event vs. forest vegetation role in NO₃-N flushing
- Multivariate statistical analyses of 17 variables defined on high-frequency data
- Predominance of forest vegetation role during baseflow conditions
- Identification of rainfall event controls of NO₃-N flushing

GRAPHICAL ABSTRACT



ARTICLE INFO

Editor: Ashantha Goonetilleke

Keywords:

Forest
Nitrate-nitrogen flushing
Rainfall-runoff formation
Rainfall events
Seasonality

ABSTRACT

Forest vegetation is a very topical research subject as part of nature-based solutions for flood protection, soil erosion, water quality improvement, etc. However, limited capabilities of such measures are rarely investigated. Therefore, in this paper, study on the interplay of the hydrometeorological and seasonal forest vegetation role in regulating the nitrate-nitrogen (NO₃-N) flushing from a forested, torrential catchment is presented. For the 43 identified rainfall events it was found that there are no statistically significant seasonal differences in NO₃-N concentrations; however, during baseflow conditions such differences were noted. The rainfall events were described by 17 hydro-meteorological and vegetation variables to investigate similarities between the events from the NO₃-N export point of view using clustering methods. Additionally, the relationship between explanatory and dependent variables, i.e. NO₃-N concentration and export variables, was modelled. In the models, the first four principal components were used as explanatory variables after the reduction of the initial number of variables. It was found that phenological phases as indicators of the forest vegetation seasonal activity are generally not able to considerably influence the NO₃-N concentration and flushing dynamics. The results indicate that during baseflow conditions, the influence of the forest vegetation in the torrential catchment becomes predominant. During rainfall events, the role of vegetation is blurred and might be generally considered as insignificant. The characteristics of rainfall events apparently exceed the limits of a forest's ability to control NO₃-N flushing. Given the pronounced impact of rainfall intensity on NO₃-N flushing, the challenge for the future will be to mitigate the potential negative effects of climate change related impacts, especially through measures able to reduce the intensity of rainfall-runoff formation. The seasonal role of vegetation in diminishing the intensity of nutrient flushing in natural torrential catchments might be relatively constrained and probably also overwhelmed by the hydrometeorological conditions.

* Corresponding author.

E-mail address: klaudija.sapac@fgg.uni-lj.si (K. Lebar).

<http://dx.doi.org/10.1016/j.scitotenv.2023.162475>

Received 3 October 2022; Received in revised form 20 February 2023; Accepted 21 February 2023

Available online 27 February 2023

0048-9697/© 2023 The Authors. Published by Elsevier B.V. This is an open access article under the CC BY-NC license (<http://creativecommons.org/licenses/by-nc/4.0/>).

1. Introduction

It is well known that forest vegetation plays an important role in the hydrological cycle and water balance. For example, one part of the rainfall is intercepted by the tree canopy and it is estimated that on the global scale this accounts for up to 50 % of the annual rainfall amounts (Roth et al., 2007). Due to the reduced rainfall that reaches the soil, runoff is reduced (e.g., Mohammad and Adam, 2010; Zabret and Šraj, 2015). Moreover, tree canopy rainfall interception decreases rainfall kinetic energy resulting in lower rainfall erosivity and soil erosion rates (e.g., Li et al., 2019). Water erosion and soil loss are also associated with the removal and flushing of nutrients such as nitrogen (e.g., Yao et al., 2021), which are essential for the growth of primary producers. There are also other tree-related processes that influence the water balance. For instance, tree roots affect infiltration rates (Zhang et al., 2019), while transpiration accounts for 39 % of global terrestrial precipitation (Schlesinger and Jasechko, 2014).

Seasonal changes in biotic activity and temporal variability of hydrological conditions make it extremely difficult to determine the prevailing factors causing increased leaching of mobile forms of nutrients (such as nitrate) from natural forested catchments. The increased flushing of nitrate can be related to increased deposits in forest soils that accumulate over longer, rainless periods due to the seasonal increase in their availability through increased mineralization and nitrification rates (Rusjan and Vidmar, 2017). Due to the interconnectedness and interdependence of the aforementioned processes, the understanding of the rainfall-runoff formation and dissolved substances transport pathways cannot rely only on hydrometeorological data and information about catchment characteristics, but also on measurements of mobile nutrient chemical forms, such as nitrate, which can be of great importance (Exner-Kittridge et al., 2016). These data enable also knowledge discovery (Aubert et al., 2016), inference about the sources of individual substances (Bernal et al., 2006), and prediction about a catchment's response from the nutrient retention and flushing points of view (Rusjan and Vidmar, 2017).

Simultaneous monitoring of nitrate-nitrogen ($\text{NO}_3\text{-N}$) concentrations and hydrological parameters (e.g., discharge) is relatively common in areas where high $\text{NO}_3\text{-N}$ concentrations pose an environmental risk (e.g., agricultural areas) (e.g., Moravcová et al., 2013; Parra Suárez et al., 2019). However, there are fewer studies examining $\text{NO}_3\text{-N}$ concentrations in relation to hydrological parameters in catchments with natural land use (e.g., forest) (e.g., Koenig et al., 2017; Snyder et al., 2018). Yet, most of the knowledge about these processes is still based on traditional data acquisition approaches, i.e. discrete sampling followed by analysis in laboratory (Pellerin et al., 2016), meaning that many rapid time-changing processes are still not sufficiently understood. Recently, plenty of studies have addressed the influence of nature-based solutions such as reforestation or conservation of forests for flood protection (e.g., Markart et al., 2021), soil erosion reduction (Teng et al., 2019), water quality improvement (Keller and Fox, 2019), etc. However, the potential limitations of such measures are rarely investigated. In this context, there is still a huge lack of knowledge about interconnection between hydrological and biogeochemical processes, triggered by rainfall characteristics, and rainfall-runoff formation patterns (Ross et al., 2021).

In this paper, a closer look at rainfall event characteristics and changes in $\text{NO}_3\text{-N}$ concentrations is provided. The main objective of the study is to investigate the interplay between the hydrometeorological conditions and the "natural" forest vegetation role in regulating the $\text{NO}_3\text{-N}$ flushing observed through high-frequency streamwater $\text{NO}_3\text{-N}$ concentration measurements in a small, undisturbed torrential catchment. More specifically, the manuscript aims to: (i) identify the most influential hydrometeorological variables on the $\text{NO}_3\text{-N}$ flushing from the small, natural torrential catchment, where additional (anthropogenic) sources of nitrate are not present, (ii) investigate the differences in the $\text{NO}_3\text{-N}$ concentrations and export amounts during particular rainfall events, and (iii) evaluate the seasonal role of vegetation on the rainfall-runoff formation and $\text{NO}_3\text{-N}$ flushing processes by taking into account hydrometeorological characteristics and $\text{NO}_3\text{-N}$ concentration variables.

2. Methodology

2.1. Study area and data description

For the study area, a small (70 ha) Kuzlovec stream catchment, central Slovenia, was selected, with steep slopes ranging between 820 and 410 m a.s.l. (Bezák et al., 2013; Sapač et al., 2020). According to land use data, >90 % of the catchment area is covered by forest (MKGP, 2018). This is followed by permanent meadows (7 %), while other land uses make up <1 % of the area (Appendix Fig. A1). The forest is classified as mixed. Among deciduous trees (65 %), beech dominates, and among conifers (35 %), spruce. In view of climate characteristics, the study catchment is located in a transitional area between sub-Mediterranean and temperate continental climates. Highest rainfall sums can be expected in fall and winter seasons. However, high-intensity, relatively short-duration rainfall events can occur especially in summer (Bezák et al., 2017a). The air temperature in a two-year monitoring period (April 2018–April 2020) ranged from -8.6 to 30.2 °C with an average annual temperature of 10.2 °C in 2019. The coldest month was January with an average monthly temperature around 0 °C, while the highest temperatures are typical for summer months (June, July, and August) (monthly averages around 20 °C).

For the evaluation of the role of forest vegetation seasonality in the formation of rainfall-runoff processes and $\text{NO}_3\text{-N}$ flushing, 20-min streamflow data, precipitation data from seven HOBO RG3-M tipping buckets (e.g., amount, intensity, duration), and data on $\text{NO}_3\text{-N}$ concentrations at the outflow of the catchment (e.g., maximum, average concentration) were obtained (Appendix Fig. A1, left). A multiparameter sonde (Hydrolab MS5) with an ion-selective sensor was used for measuring streamwater $\text{NO}_3\text{-N}$ concentrations. According to the manufacturer, the measurement range of the $\text{NO}_3\text{-N}$ sensor is $0\text{--}100$ mg/l with ± 5 % accuracy and 0.01 resolution. In order to assure accurate water chemistry readings of the sonde, maintenance and calibration procedures were carefully followed. Moreover, field water samples were collected biweekly and analysed in the laboratory in order to control the multiparameter sonde readings. In addition, data on three-day cumulative reference evapotranspiration prior the rainfall event from the nearest relevant weather station were obtained (ARSO, 2020) and the number of previous days without precipitation were calculated. Forest vegetation seasonality was determined according to the leaf area index (LAI) periodic measurements using LAI-2200C Plant Canopy Analyzer in combination with analyses of MODIS Terra satellite images (Čotar et al., 2018; Ogris et al., 2018). More specifically, the annual forest vegetation dynamics was determined based on the methodology presented by Zhang et al. (2003), who calculated transition dates of four phenological phases, i.e. green-up, maturity, senescence, and dormancy. Detailed data on hydrometeorological and concentration variables were available for the period April 2018–April 2020, in which 43 rainfall events were covered. A rainfall event was defined arbitrarily by considering the minimum cumulative rainfall amount of 10 mm. During all identified events, an increase in discharge from 0.2 to 68.8 l/s was observed. Even the events in the growing season, with rainfall sums around 10 mm, caused a stream discharge increase from 0.2 to 11.2 l/s. The average discharge in the observed period was 4.5 l/s, based on 20-min data. A similar criterion was also used by other authors (e.g. Huebsch et al., 2014). Two events were separated by at least a 6-h rainless period (Bezák et al., 2017b; Sapač et al., 2020). The studied catchment is torrential with steep slopes resulting in high streamflow velocities and turbulence and susceptible to flash floods (Mikoš et al., 2002; Heiser et al., 2015). Therefore, the relevance of the selected criteria could be confirmed also by data visualization (quick return of the discharges to the pre-event values). The fast hydrological response of the studied catchment to rainfall events also highlights the need to use high-frequency data in order to be able to observe both hydrological conditions and related $\text{NO}_3\text{-N}$ concentration changes. Due to the relatively limited sample size, the annual dynamics of forest vegetation was divided into two seasons. On average, the growing season (period of green-up and maturity) started on 27 March and ended on 12 September, while the non-growing season (period of senescence and dormancy) was defined for

the rest of the year. The seasons were compared in terms of the catchment's response to rainfall events and NO₃-N exports both in rainfall event and no-event periods.

In the presented analyses, 17 variables were determined to characterise and discretise the rainfall events, associated changes in stream discharge, NO₃-N concentrations, and forest vegetation seasonal characteristics (Table 1). The values of the selected variables assured that the 43 identified rainfall events covered very different hydrological (e.g. rainfall events characteristics, stream discharge temporal changes) and seasonal vegetation conditions. Moreover, the variables describing changes of NO₃-N concentration varied considerably between the events. For example, on average, a rainfall event lasted 900 min, with a temporal span between 20 and 3040 min. The highest recorded rainfall sum/event was 95 mm, with the mean and median values of 32.1 and 24.3 mm, respectively. Rainfall kinetic energy is an important factor controlling the soil erosion processes and rainfall-runoff formation. The rainfall kinetic energy (*E*) was therefore calculated using empirical equation suggested by Brown and Foster (1986) where *E* varies with rainfall intensity. The highest *E* was calculated for a 20-min event on 2 August 2019 (15.4 MJ/(ha mm)). In this respect, especially for such extreme events, data with a short time step of measurement are important. Due to the topography (steep terrain) and erodibility of the geological base, the selected catchment is prone to soil erosion (e.g., Bezak et al., 2017a). Moreover, according to the soil analysis in the catchment, the top (soil depth up to 20 cm) and middle (soil depth up to 50 cm) soil layers (most prone to rain-induced erosion) represent the main storage of the total nitrogen and NO₃-N. The topsoil layers have a pH value around 6.5; the pH values increase to 7.7 in deeper soil layers. In view of the carbon-to-nitrogen ratio (C/N) as an indicator of forest soils susceptibility for NO₃-N leaching (e.g., Gundersen et al., 1998; Lovett et al., 2002), lower C/N ratios (between 12 and 15) were calculated for the upper soil layers (soil depths up to 50 cm) and higher ratio values (24.5) for deeper soil layers. The maximum discharges (*Q*_{max}) during events ranged from 2.0 to 75.9 l/s (Fig. 1), while the mean concentration and mean export of NO₃-N ranges were 0.6–3.0 mg/l and 0.1–1.3 g/min, respectively.

2.2. Statistical analysis

To investigate and describe the characteristics of the 43 rainfall events, commonly applied multivariate exploratory statistical methods, namely hierarchical clustering (Ward's method on squared Euclidean distances) and k-means, were used on 17 pre-defined variables (Table 1). Additionally, 11 variables describing characteristics of rainfall events and hydrological conditions in the catchment (*Pa*, *Pd*, *Imean*, *I60*, *E*, *ET3*, *Qmax*, *Qi*, *Qr*, *N_days*, *LAI*) were used in the principal component analysis (PCA) to obtain the most important PCs, which were further included in the multiple linear regression models for explaining the dynamics of NO₃-N flushing described

by the variables, *C_{rc}*, *C_{max}*, *C_{mean}*, *Cr*, *Exp_{mean}*, and *Exp_{max}* (Table 1). The first four variables (*C_{rc}*, *C_{max}*, *C_{mean}*, *Cr*) represent the changes in concentrations during rainfall events, whereas the last two (*Exp_{mean}*, *Exp_{max}*) represent the variables of the amount of flushed NO₃-N masses (concentration multiplied by discharge).

The PCA was used to reduce the number of explanatory variables. In contrast to clustering, PCs are extracted to identify the patterns determined by the amount of variance in the dataset and not to maximize the differences between groups of rainfall events. However, in case of a high number of variables, the results of both methods may lead to similar conclusions because the first principal components are usually determined by the same variables that divide a dataset into clusters.

After PCA, the multiple linear regression (MLR) was applied to model the relationship between explanatory variables and dependent variables (i.e. NO₃-N concentration and export variables). As explanatory variables, only the first PCs with eigenvalue >1 (Kaiser rule) were used, thereby reducing the number of explanatory variables, but still taking into account all meteorological, hydrological, and vegetation rainfall event characteristics. The estimation of MLR model parameters is followed by regression diagnostics (Kassambara, 2018) in order to evaluate the model assumptions and to explore whether the datasets, based on which the parameters of the model are estimated, do not include individual data that could significantly influence the value of the independent variable (i.e. influential points). All statistical analyses were made in R Studio (R Core Team, 2018).

3. Results and discussion

Since one of the goals of this research was to evaluate the role of the forest vegetation on the NO₃-N flushing, preliminary analysis was made by separating NO₃-N concentration data firstly into rainfall event periods and a reference period (the remaining time). Secondly, the data were further divided according to the phenological phases, i.e. growing and non-growing seasons (Fig. 2). It can be noticed that in the no-event period, the mean value as well as the interquartile range are lower in the growing season (spring, summer months) (Fig. 2, left). The average NO₃-N concentration in the growing period was 0.76 (±0.19) mg/l, while in the non-growing period it was 1.06 (±0.56). 50 % of the concentration measurements (interquartile range) in the growing and non-growing periods had values 0.66–0.87 mg/l and 0.86–1.18 mg/l, respectively. Similarly, for the exported masses of NO₃-N (in grams), the average export was 0.11 (±0.05) g/min and 0.14 (±0.07) g/min during growing and non-growing seasons, respectively. During the rainfall events (Fig. 2, right), small differences in mean NO₃-N concentrations during growing (1.14 ± 0.46 mg/l) and non-growing (1.13 ± 0.58 mg/l) periods could be observed with a slightly higher standard deviation and coefficient of variation in the reference period. However, the average exported NO₃-N mass was 0.23 ±

Table 1

Variables considered in the data analysis with corresponding values of mean, standard deviation, maximum, minimum, and median for 43 analysed rainfall events. Variables in italic (the last six rows) were used as dependent variables in the principal component regression analysis.

Variable [units]	Abbrev.	Mean ± std. dev.	Max.	Min.	Median
Precipitation duration [min]	<i>Pd</i>	964.2 ± 704.6	3040.0	20.0	760.0
Precipitation amount [mm]	<i>Pa</i>	32.1 ± 21.4	95.0	10.0	24.3
Mean precipitation intensity [mm/h]	<i>Imean</i>	3.7 ± 5.8	34.2	0.6	2.0
Max. 60-minute precipitation intensity [mm/h]	<i>I60</i>	15.9 ± 14.4	85.5	2.7	10.2
Kinetic energy of the rainfall event [MJ/(ha mm)]	<i>E</i>	4.3 ± 3.2	15.4	1.2	3.2
Initial discharge [l/s]	<i>Qi</i>	3.8 ± 1.8	8.3	0.8	3.6
Max. discharge [l/s]	<i>Qmax</i>	11.8 ± 13.6	75.9	2.0	8.1
Discharge range [l/s]	<i>Qr</i>	8.0 ± 13.0	68.8	0.2	4.1
Number of days without precipitation with >10 mm [days]	<i>N_days</i>	8 ± 10.3	53.2	0.3	4.1
Cumulative three-day evapotranspiration [mm]	<i>ET3</i>	7.2 ± 5.2	16.8	1.0	6.4
Leaf area index [m ² /m ²]	<i>LAI</i>	2.4 ± 2.0	4.8	0.0	1.1
<i>Relative change of NO₃-N concentration [mg/l]</i>	<i>C_{rc}</i>	20.8 ± 17.2	62.9	-14.4	22.3
<i>Max. NO₃-N concentration [mg/l]</i>	<i>C_{max}</i>	1.4 ± 0.7	3.5	0.8	1.2
<i>Mean NO₃-N concentration [mg/l]</i>	<i>C_{mean}</i>	1.2 ± 0.5	3.0	0.6	1.1
<i>Range of NO₃-N concentration [mg/l]</i>	<i>Cr</i>	0.6 ± 0.5	2.3	0.0	0.4
<i>Mean export of NO₃-N per minute [g]</i>	<i>Exp_{mean}</i>	0.4 ± 0.3	1.3	0.1	0.3
<i>Maximum export of NO₃-N per minute [g]</i>	<i>Exp_{max}</i>	0.9 ± 0.9	4.1	0.1	0.6

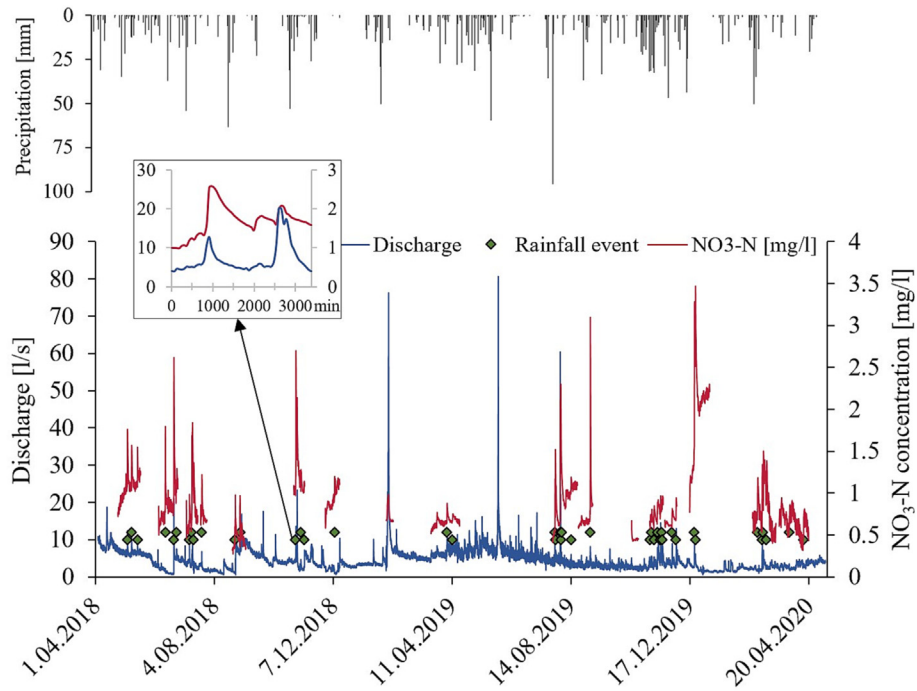


Fig. 1. Precipitation (above), discharge (blue line) and NO₃-N concentration in period April 2018–April 2020. Rainfall events are marked with green points. Discharge and NO₃-N concentration are plotted based on 20-min measurements. Precipitation is plotted based on the daily sums. (For interpretation of the references to colour in this figure legend, the reader is referred to the web version of this article.)

0.28 g/min and 0.43 ± 0.47 g/min in the growing and non-growing periods, respectively. According to the average export rates during rainfall events and baseflow period, it is expected that, on average, 1.2 kg/ha/year NO₃-N is flushed from the catchment. The total duration of the rainfall events in the period of observations represents about one-tenth of a year;

however, in this short period 30 % of the annual exported amount is flushed. Based on this initial analysis, it was further investigated if and how the nitrate flushing dynamics during different phenological phases is conditioned by the hydrometeorological characteristics of rainfall events.

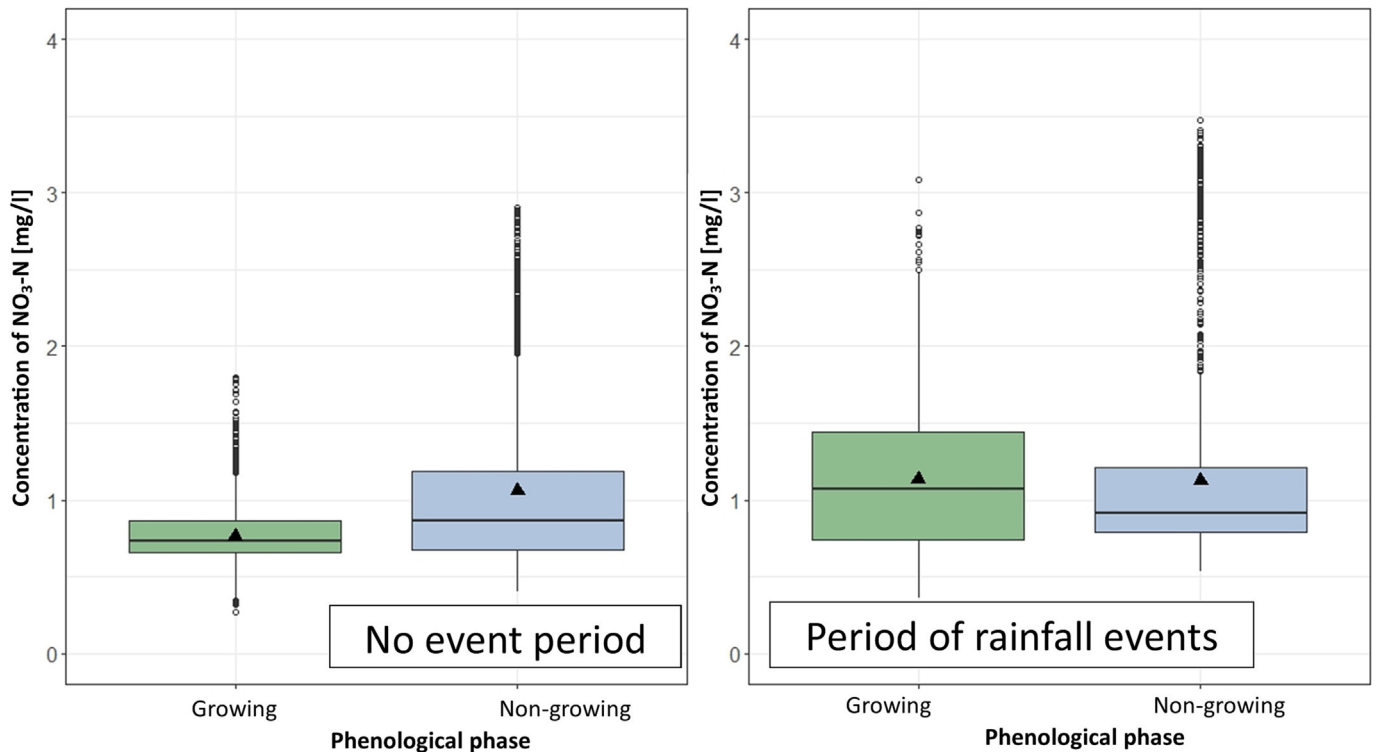


Fig. 2. Comparison of 20-min NO₃-N concentrations distribution in growing and non-growing seasons during the reference period (left) and during the periods of rainfall events (right). The triangles in the boxplot show the mean values.

3.1. Characteristics of rainfall events

The aim of the hierarchical clustering was to investigate the similarity between the rainfall events. The rainfall events were described with 17 variables (Table 1). Results of the hierarchical clustering are presented with the informative heatmap (Appendix Fig. A2) that suggests that there are four optimal clusters into which the events are merged. The same set of variables was further used in k-means clustering using the suggested number of clusters ($k = 4$). Results of k-means confirmed the suggested number of clusters as optimal. All the individual rainfall events were merged into the same clusters as with hierarchical clustering, except for one event.

For the two events, i.e. from 1 February 2019 and the earlier one from 2 August 2019, grouped in cluster 1, high mean and maximum amounts of flushed $\text{NO}_3\text{-N}$ (Exp_mean , Exp_max) as well as high peak discharges ($Qmax$) are characteristic (Fig. 3). Fig. 3 The events in cluster 2 have in common high concentrations of $\text{NO}_3\text{-N}$ (mean, maximum, and absolute change), although the events occurred in different seasons and, consequently, in different phenological conditions. The main difference between clusters 3 and 4 is especially noticeable for variables $ET3$ and LAI . These two variables have a distinct seasonal variability, so it is not surprising that all events in cluster 3 occurred during the growing season and most events from cluster 4 in the non-growing season. In cluster 4, four out of 20 events occurred in the growing season according to the defined periods of phenological phases. A closer look at these events shows that three of them occurred at the transition from one phenological phase to another in spring (10 April 2019, 14 April 2020, and 30 March 2020) and one in the middle of the growing season (25 August 2018). The latter event was characterized by a large amount of rainfall and long duration, which are characteristics of autumn-winter rainfall events (Kobold and Sušelj, 2004). Regardless of the clear differences of seasonal variables between clusters 3 and 4, such an obvious contrast is not noticeable for the variables used to describe the temporal dynamics of $\text{NO}_3\text{-N}$ concentration and exported amounts. These results suggest that the period of the year in which the event occurred (seasonality) is not a direct indicator of $\text{NO}_3\text{-N}$ concentration variability or exported amounts during a particular rainfall event (Fig. 3, bottom row).

3.2. Reduction of the explanatory variables

In PCA of all explanatory variables, 83.5 % of variability was explained with the first four PCs having an eigenvalue greater than one. According to the loadings of the original variables (Fig. 4), to the first principal component (PC1), kinetic energy of rainfall (E), absolute change of the discharge (Qr) and peak discharge ($Qmax$), amount of precipitation (Pa), and maximum 60-minute rainfall intensity ($I60$) contribute the most. PC1 can be therefore considered as a measure of event intensity (Fig. 4). The second principal component PC2 is a measure for seasonality since the highest loadings correspond to $ET3$ and LAI , both positively correlated to PC2. PC2 is positively correlated also with I_{mean} and negatively with Pd . PC3 and PC4 can be described as principal components indicating the influence of antecedent conditions due to high correlation with the initial (pre-event) discharge (Qi) and the number of rainless days before the event (N_days), respectively. Higher positive or negative loadings mean a higher positive or negative correlation between the variable and the PC, respectively.

Additional information on the role of the forest vegetation during rainfall events on rainfall-runoff formation and consequent $\text{NO}_3\text{-N}$ flushing could be provided by combining the results of k-means clustering and PCA (Fig. 4). Results in the PC1-PC2 and PC3-PC4 planes are shown (Fig. 4). Based on the centroids of the individual cluster in the PC1-PC2 plane, one can see that events with a larger change of discharge (Qr) and maximum discharge ($Qmax$) are characteristic for cluster 1 (yellow dots) (Fig. 4, left). All the events merged into cluster 3 are on the upper half of the vertical axis (PC2), whereas events from cluster 4 are in the bottom half of PC2. As PC2 is the most correlated with the previous three-day evapotranspiration ($ET3$) and leaf area index (LAI), it can be concluded that events of cluster 3 occurred in the period with higher LAI and $ET3$, i.e., late spring and summer months. The opposite is suggested for the events of cluster 4. Events with higher mean rainfall intensity are characteristic for cluster 3. PC2 is determined also by the rainfall duration (Pd). In this context, for cluster 3, rainfall events with longer rainfall duration are characteristic compared to events grouped in cluster 4. The most non-homogenous cluster in the PC1-PC2 plane is cluster 2; this cluster merges

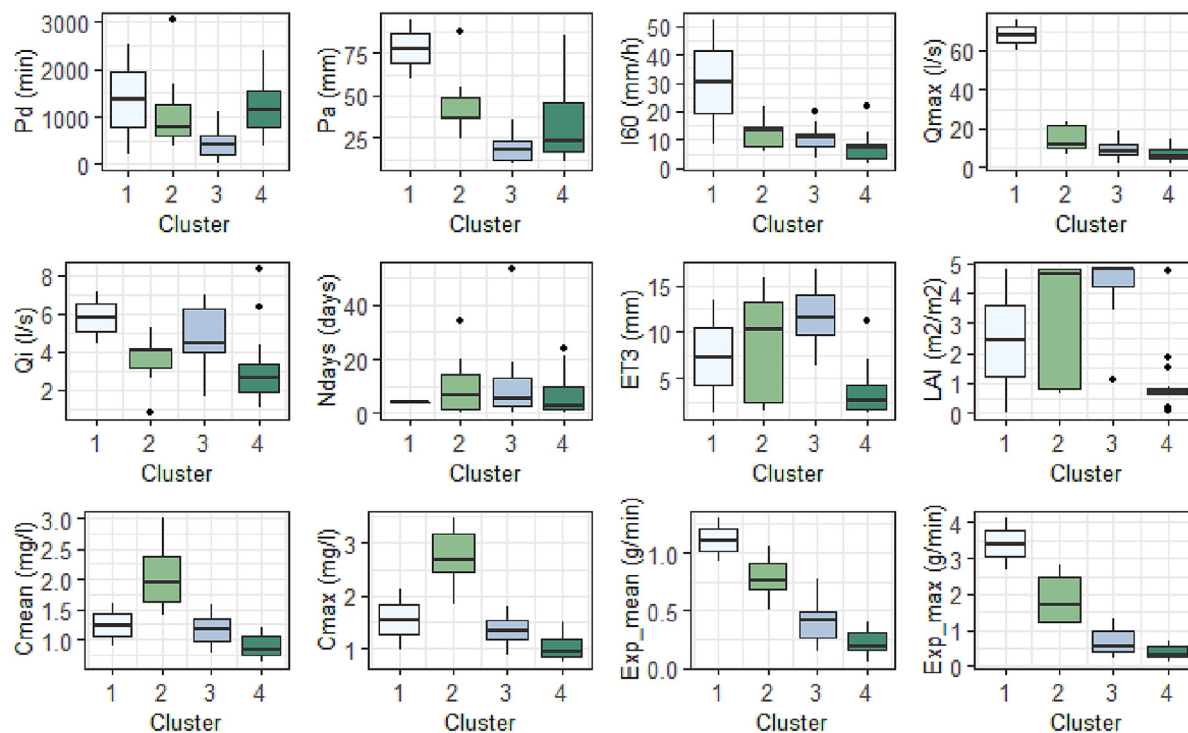


Fig. 3. Distribution of the selected variable values included in the cluster analysis performed by k-means clustering into four groups. The first two rows show the distribution of hydrological and vegetation variable values in the individual clusters. The bottom row shows the distribution of dependent ($\text{NO}_3\text{-N}$ -related) variable values in the individual clusters.

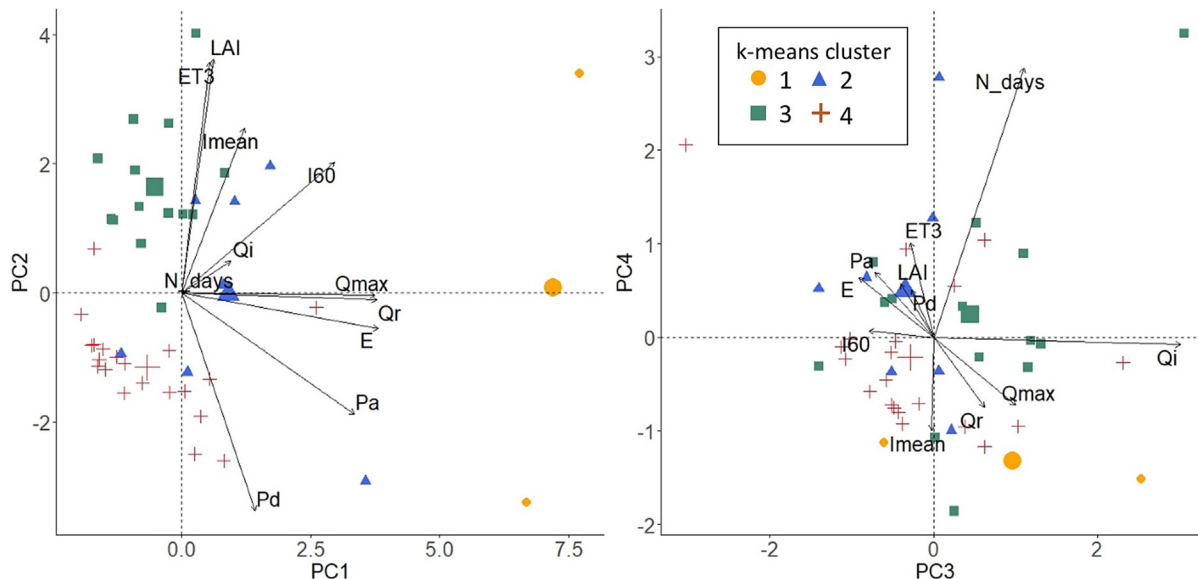


Fig. 4. Biplot of the principal component analysis of 11 hydro-meteorological variables in the PC1-PC2 space (left) and the PC3-PC4 space (right). Rainfall events (PC scores) are coloured according to the k-means clusters (groups). Centroids of each cluster (group) are shown by a larger symbol of the corresponding colour. The length of the individual variable vector (loading) reflects the contribution to the individual PC. The events on the same side as the individual variable vector have higher values of this variable than the events on the opposite side.

events with higher concentrations and amounts of exported $\text{NO}_3\text{-N}$. Based on these findings and results of the clustering methods, it may be concluded that the occurrence of events with high concentrations of $\text{NO}_3\text{-N}$ cannot be unambiguously explained solely by 11 considered hydrometeorological and vegetation variables. In other words, increased $\text{NO}_3\text{-N}$ concentrations can occur under contrasting hydrometeorological and seasonal (phenological phase) conditions. The results somewhat contradict the recent findings by Winter et al. (2022b), who primarily focused on the C-Q hysteresis loop as an indicator of $\text{NO}_3\text{-N}$ flushing. For the Kuzlovec stream torrential catchment, even the statistical test of differences between the indicators of hysteresis loops did not show statistically significant differences between seasons (Sapač et al., 2021). Additionally, one of the indicators, namely the ratio of coefficient of variation of $\text{NO}_3\text{-N}$ concentration and discharge, was shown to be most likely related to seasonal variability in the characteristics of rainfall events rather than to changes in the phenological phases of the forest vegetation in the catchment. Similar conclusions as those from PC1-PC2 can be drawn from the PC3-PC4 plane (Fig. 4, right).

3.3. Modelling the relation between $\text{NO}_3\text{-N}$ and explanatory variables

The first four principal components (PC1, PC2, PC3, PC4) were used as explanatory variables in multiple linear regression (MLR) models for dependent variables: C_{mean} , C_{max} , Cr , C_{rc} , Exp_{mean} , and Exp_{max} . Based on the MLR models, only the relationships between PCs and the three dependent variables, i.e. Cr , Exp_{mean} , and Exp_{max} , are statistically significant (Table 2). Results of the MLRs indicate that with the first four PCs 33 %, 57 %, and 69 % of the Cr , Exp_{mean} , and Exp_{max} variance is explained, respectively. This is most likely due to the wide range of rainfall event characteristics (from small to large amounts of rainfall, short and long durations, various rainfall intensities, etc.) described by 11 variables in a statistically relatively limited sample. Consequently, the prediction of complex dependent variables such as $\text{NO}_3\text{-N}$ concentrations based on the rainfall characteristics appears to be unreliable. On the other hand, the relatively successful prediction of export variables could be associated to the strong correlation between discharge and exported amounts. In the models for the mean and maximum exported amount of $\text{NO}_3\text{-N}$ (Exp_{mean} , Exp_{max}), PC1 and PC3 variables are statistically significant (Table 2). These PCs are related with the rainfall event intensity (Q_{max} , Q_r , Pa , I_{60} , E) and initial hydrological conditions (Q_i) the most. According to the linear

regression model diagnostic based on residuals plots, the event from 25 August 2018 proved to be an influential point in all three regression models (Cr , Exp_{mean} , Exp_{max}), while in the model for Exp_{max} the event from 2 August 2019 was also identified as an influential point. The influential events could be characterized by a high kinetic energy, rainfall intensity, and the amount of rainfall. However, Exp_{max} in these events was considerably lower than in comparable events. Results of the MLR models without identified influential points are shown in Table 2 in rows with suffix “B”. The proportion of variance explained by the models without influential points did not change in case of model for Exp_{mean} (57 %), while in case of Cr and Exp_{max} it increased to 51 % and 76 %, respectively.

After excluding the influential points (rainfall events), statistical significance of PC1 and PC3 remains the same in the model for Exp_{mean} , while in the model for Exp_{max} , PC3 is no longer statistically significant (Table 2). The removal of influential points results in all four PCs as statistically significant for the explanation of the absolute change of $\text{NO}_3\text{-N}$ concentration (Cr) during a rainfall event (Table 2). However, the coefficient of determination of the Cr model is considerably lower than for Exp_{mean} and Exp_{max} models, which may be a consequence of the complexity of the processes reflected in $\text{NO}_3\text{-N}$ concentration related variables. In the Cr model, the highest change of the estimated parameter is found for the PC3 variable, which is characterized with initial conditions, namely with initial discharge (Q_i), and for PC4, which is related with the number of previous rainless days (N_{days}). In other words, the lower the Q_i and the longer the rainless period, the higher the expected change of $\text{NO}_3\text{-N}$ concentration, considering other PCs in the MLR. From the process point of view, this might be

Table 2

Results of the multiple linear regression model based on the first four principal components for Exp_{mean} , Exp_{max} , and Cr . The rows with suffix »B« in the first column show the results without identified influential points.

Model	PC1	PC2	PC3	PC4	R ²
Exp_mean	***		**		0.57
Exp_mean_B	***		**		0.57
Exp_max	***		*		0.69
Exp_max_B	***				0.76
Cr	**		+	*	0.33
Cr_B	***	+	**	***	0.51

Level of statistical significance: ***0.001; **0.01; *0.05; + 0.1

related to accumulation of $\text{NO}_3\text{-N}$ in forest soils due to the absence of rainfall-runoff formation mechanisms that are able to mobilize $\text{NO}_3\text{-N}$ towards the streams. In this context, in the recent study by Winter et al. (2022a) who investigated $\text{NO}_3\text{-N}$ export during droughts in 2018 and 2019, it was shown that rewetting after dry period results in higher in-stream $\text{NO}_3\text{-N}$ peaks. They attributed higher $\text{NO}_3\text{-N}$ export amounts to reduced denitrification due to lower soil water content in prolonged rainless periods, which leads to accumulation of inorganic nitrogen forms in catchment soils flushed away during rainfall events, and to decreased plant uptake. The influence of hydrological antecedent conditions was investigated also by Blaes et al. (2017), who clearly demonstrated the role of hydrological antecedent conditions in the nitrate concentrations.

Plots in Fig. 5 show the predicted values for Exp_{max} , Exp_{mean} , and Cr in dependence on each PC at the average value of other three PCs. For each of these variables, the relation with principal components (PC1–PC4) is shown with the regression line and the corresponding 95 % confidence interval for the average prediction. For all three variables one can note that PC1 has the highest influence on their values. The relation is positive confirming that more intense rainfall events cause a larger change of $\text{NO}_3\text{-N}$ concentration (Cr) and larger amounts of exported $\text{NO}_3\text{-N}$ (Exp_{mean} , Exp_{max}). Other PCs have less impact on the response variables. This is especially pronounced for the Exp_{max} variable (Fig. 5, top row) where regression lines are almost parallel to the horizontal axis. Among other three PCs, PC3, which is determined with the initial discharge at the beginning of the event (Qi), identifies the second greatest impact on the Exp_{mean} variable with a positive relation. However, a negative relation with PC3 is identified with

the Cr variable (Fig. 5, bottom row), suggesting that the lower Qi results in a higher concentration change during the rainfall event. For highly torrential small catchments, this suggests that prolonged rainless periods, when due to the absence of rainfall-runoff processes $\text{NO}_3\text{-N}$ may accumulate in soils, might be one of the main conditions necessary for an increased change of $\text{NO}_3\text{-N}$ concentration during a rainfall event. The role of the antecedent rainless periods could be further supported by the relatively limited capacity of the forest soils in the studied catchment (according to the analysed soil C/N ratios) to diminish the $\text{NO}_3\text{-N}$ export. Seasonality is expressed with PC2 that, interestingly, did not prove to be influential on Exp_{mean} and Exp_{max} (Fig. 5). However, its influence is noticeable in case of Cr (Fig. 5). In the seasonal context, prediction models suggest that one can expect higher $\text{NO}_3\text{-N}$ concentration changes during events with a shorter duration and larger three-day evapotranspiration and leaf area index. Such events are typical for the summer months (growing phase) when mineralization and consequent accumulation of $\text{NO}_3\text{-N}$ in soils is also intensified (Winter et al., 2022a). During a rainfall event, the accumulated soil $\text{NO}_3\text{-N}$ could be available to be mobilized towards the stream network. Additionally, a greater absolute change in streamwater $\text{NO}_3\text{-N}$ concentration after prolonged dry periods can be also attributed to lower $\text{NO}_3\text{-N}$ concentration during rainless conditions in the growing season before the rainfall event (Fig. 2) resulting from higher plant uptake (Winter et al., 2022a) and/or disconnection of shallow flow paths and therefore nitrate transport towards the stream, similarly as suggested by Yang et al. (2018).

The role of the forest and, more specifically, its phenological phases in the $\text{NO}_3\text{-N}$ export dynamics on rainfall event basis was proven to be

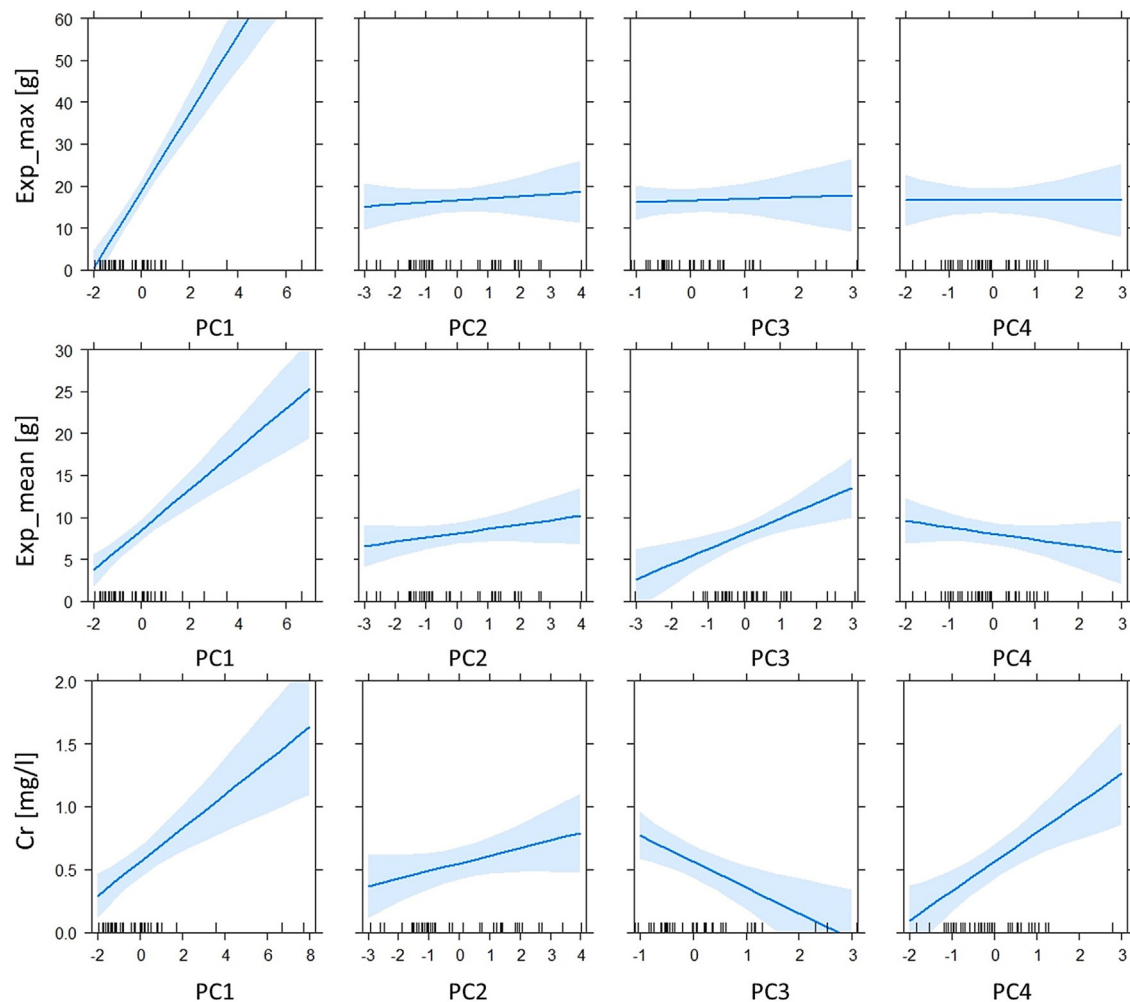


Fig. 5. Predicted values of Exp_{max} , Exp_{mean} , and Cr (blue solid line) with 95 % confidence intervals (light blue area) for mean model prediction considering all other explanatory variables in the model. (For interpretation of the references to colour in this figure legend, the reader is referred to the web version of this article.)

important in some previous studies. Rusjan and Mikoš (2008) explained the seasonal difference in the dynamics of $\text{NO}_3\text{-N}$ concentrations based on pre-vent air temperatures and soil moisture conditions that influence the processes of forest soil mineralization and nitrification. Similar was reported by Arheimer et al. (1996). In view of the seasonal influences on the soil N storage, higher mineralization and nitrification rates are expected during the growing period when temperatures are high, while the highest availability of $\text{NO}_3\text{-N}$ for flushing could be expected in autumn and winter when the forest vegetation N uptake is considerably reduced, as discussed by, e.g., Casson et al. (2014) in similar climate conditions. However, in the studied catchment, the dynamic change in the soil $\text{NO}_3\text{-N}$ storage between the growing and non-growing periods might be constrained due to the flushing character of the studied torrential catchment, which appears to limit the ability of forest soils to accumulate $\text{NO}_3\text{-N}$ to a greater extent. More specifically, data of this study show that small rainfall events (rainfall sums of 10–15 mm) cause an increase in discharge and are able to trigger $\text{NO}_3\text{-N}$ flushing regardless of the seasonal conditions.

The clustering of rainfall events indicated the influence of seasonality (*ET3*, *LAI*) for most of the events (34 out of 43). However, interestingly, events with the highest recorded $\text{NO}_3\text{-N}$ concentrations and $\text{NO}_3\text{-N}$ export were merged in the other two clusters where seasonality was not influential (i.e., events occurred in different parts of the year). This was also confirmed with MLR models using PCs as explanatory variables, where hydrometeorological characteristics of a rainfall event combined into PC1 (amount and intensity of precipitation, discharge) proved to be statistically significant for explaining *Exp_{mean}* and *Exp_{max}*. The influence of seasonal conditions (PC2) was observed only in case of absolute change of $\text{NO}_3\text{-N}$ concentration. On the other hand, the comparison of statistical values (e.g., mean, median, interquartile range) of $\text{NO}_3\text{-N}$ concentrations and exported amounts between rainfall events and in the reference period (baseflow conditions) showed a seasonality effect during baseflow, while there are no considerable differences between phenological phases during rainfall events. Similar seasonal differences during baseflow conditions were reported also by Sebestyen et al. (2014) based on weekly sampling. Feinson et al. (2016) applied C-Q hysteresis loops for identifying the seasonality effect during rainfall events at different locations. They found that for size and direction of the hysteresis loop, seasonality is a statistically significant variable in the linear model only in the interaction with the location variable. In some studies, snow and snow cover were identified as important factors influencing the amount of exported nitrogen (e.g., Brooks et al., 1999). Therefore, for the catchments with longer presence of winter snow cover, during the spring snowmelt the highest amounts of nitrogen are exported from accumulated nitrogen sources in the snow as well as from microbial produced nitrogen in the soil (Judd et al., 2007). In our dataset, there was no snow cover and the rainfall events were occurring relatively regularly. Hence, it can be presumed that the $\text{NO}_3\text{-N}$ was not able to accumulate to a greater extent in the forest soils in the colder part of the year and be available for export during the following rainfall events, as it would have been expected after a prolonged presence of snow cover. According to Slovenian Environment Agency (ARSO, 2017), in the period 1961–2011 the total snow cover in Slovenia decreased by 55 %, while the height of the freshly fallen snow decreased by 40 %. Moreover, it is expected that due to the impact of climate change, the largest increase in air temperature will be in the wintertime. This might indicate that in the future even less snow cover is expected, which will also lead to an overall lower retention capability of nutrients in the soils during the winter. No change in the total annual amount of precipitation is expected in the future, but changes in seasonal variability can be expected, especially with larger rainfall sums in winter. This could mean that the $\text{NO}_3\text{-N}$ from torrential catchments with a natural (forest) cover, such as the one investigated in this study, would be regularly flushed away, while the amount of accumulated $\text{NO}_3\text{-N}$ in the soil could be even lower. Consequently, the forest vegetation $\text{NO}_3\text{-N}$ retention capacity could be further reduced by the changing hydrometeorological conditions.

The seasonal role of forest vegetation in $\text{NO}_3\text{-N}$ concentrations was identified just in reference, prolonged periods of baseflow conditions

where significant differences in $\text{NO}_3\text{-N}$ concentrations were observed. During rainfall events, seasonal differences in $\text{NO}_3\text{-N}$ concentrations that could be associated to the activity of the forest vegetation were not identified. Generally, the results of multivariate analyses presented in this study suggest that the hydrometeorological conditions, expressed by the characteristics of rainfall events (especially rainfall intensity and rainfall amount), prevail over the expected seasonal impact of the forest on streamwater $\text{NO}_3\text{-N}$ concentrations and consequent flushing. This indicates the limited ability of the forest vegetation to regulate $\text{NO}_3\text{-N}$ flushing amounts in small catchments with prevailing torrential characteristics. In this respect, our results could be helpful in providing important information for planning possible measures to mitigate the negative effects of climate change impacts on nutrient exports to water bodies as well as a reference state for assessing and comparing nutrient flushing processes from areas with elevated nutrient inputs (e.g., agricultural areas).

Natural (forest) vegetation is usually considered to be one of the crucial elements of nature-based solutions able to mitigate the potentially negative effects of altered hydrometeorological conditions on increased nutrient flushing. In view of the climate change projections by the end of the 21st century, further research on the role of hydrometeorological conditions on the $\text{NO}_3\text{-N}$ exports should be done to increase the knowledge of the multi-function role and potential limitations of nature-based solutions.

4. Conclusions

Research on the interplay of hydrometeorological and seasonal conditions affecting $\text{NO}_3\text{-N}$ flushing from a small, forested catchment has highlighted the complexity of the processes, showing that the role of individual variables cannot be unambiguously identified without considering the others. Still, some important messages can be drawn:

- Seasonal forest vegetation role is not able to considerably influence the $\text{NO}_3\text{-N}$ concentration dynamics and flushing during rainfall events due to the dominant role of the flushing processes.
- During rainless period, the seasonal influence of the forest vegetation in the catchment becomes prevailing, which is reflected in significant seasonal differences in stream $\text{NO}_3\text{-N}$ concentrations.
- Given the pronounced impact of the rainfall intensity on the $\text{NO}_3\text{-N}$ flushing, the challenge for the future will be how to mitigate the potential negative effects of the climate change related impacts, especially through measures able to reduce the intensity of rainfall-runoff formation processes (e.g. by an improved understanding of the forest vegetation role and limitations when implementing different nature-based solutions).
- High-frequency measurements of hydrometeorological conditions and nutrient concentrations, similar as the ones presented in this study, are crucial to improve understanding of the interplay between the hydrometeorological conditions and seasonal vegetation role, related also to the impact of different land uses in regulating the nutrient exports to water bodies.

Supplementary data to this article can be found online at <https://doi.org/10.1016/j.scitotenv.2023.162475>.

CRedit authorship contribution statement

Conceptualization (K.L., S.R., D.K.); Data curation (K.L.); Formal analysis (K.L.); Funding acquisition (S.R.); Investigation (K.L.); Methodology (K.L., D.K.); Supervision (S.R.); Validation (D.K.); Visualization (K.L.); Roles/Writing - original draft (K.L.); Writing - review & editing (K.L., D.K., S.R.).

Data availability

Data will be made available on request.

Declaration of competing interest

The authors declare that they have no known competing financial interests or personal relationships that could have appeared to influence the work reported in this paper.

Acknowledgments

The authors acknowledge that the research was financially supported by the Slovenian Research Agency, PhD grant of the first author, research core funding No. P2-0180, and research projects No. J6-4629 and No. N2-0313. The activities of the research are partially co-financed by the Slovenian Research Agency and by the Slovenian Ministry of Education, Science and Sport under UNESCO's Intergovernmental Hydrological Programme. Research activities were conducted in the scope of the UNESCO Chair on Water-related Disaster Risk Reduction.

References

- Arheimer, B., Andersson, L., Lepistö, A., 1996. Variation of nitrogen concentration in forest streams - influences of flow, seasonality and catchment characteristics. *J. Hydrol.* 179 (1–4), 281–304.
- ARSO, 2017. Ocena podnebnih sprememb v Sloveniji do konca 21. stoletja, Ljubljana. available at: http://www.meteo.si/uploads/probase/www/climate/text/sl/publications/OPS21_Porocilo.pdf.
- ARSO, 2020. Reference evapotranspiration and precipitation from automatic stations (daily data since 2017). available at: https://meteo.arso.gov.si/met/sl/agromet/data/arhiv_etp/.
- Aubert, A.H., Thrun, M.C., Breuer, L., Ullsch, A., 2016. Knowledge discovery from high-frequency stream nitrate concentrations: hydrology and biology contributions. *Sci. Rep.* 6 (July), 1–8 Nature Publishing Group.
- Bernal, S., Butturini, A., Sabater, F., 2006. Inferring nitrate sources through end member mixing analysis in an intermittent Mediterranean stream. *Biogeochemistry* 81 (3), 269–289.
- Bezák, N., Grigillo, D., Urbančič, T., Mikoš, M., Petrovič, D., Rusjan, S., 2017a. Geomorphic response detection and quantification in a steep forested torrent. *Geomorphology* 291, 33–44.
- Bezák, N., Rusjan, S., Kramar Fijavž, M., Mikoš, M., Šraj, M., 2017b. Estimation of suspended sediment loads using copula functions. *Water* 9, 628. <https://doi.org/10.3390/w9080628>.
- Bezák, N., Šraj, M., Rusjan, S., Kogoj, M., Vidmar, A., Sečnik, M., Brilly, M., et al., 2013. Primerjava dveh sosednjih eksperimentalnih hudourniških porečij: Kuzlovec in Mačkov graben = Comparison between two adjacent experimental torrential watersheds: Kuzlovec and Mačkov graben. *Acta Hydrotech.* 45 (2013), 85–97.
- Blaen, P.J., Khamis, K., Lloyd, C., Comer-Warner, S., Ciocca, F., Thomas, R.M., MacKenzie, A.R., et al., 2017. High-frequency monitoring of catchment nutrient exports reveals highly variable storm event responses and dynamic source zone activation. *J. Geophys. Res. Biogeosci.* 122 (9), 2265–2281.
- Brooks, P.D., Campbell, D.H., Tonnessen, K.A., Heuer, K., 1999. Natural variability in N export from headwater catchments: snow cover controls on ecosystem N retention. *Hydrol. Process.* 13 (14–15), 2191–2201.
- Brown, L.C., Foster, G.R., 1986. Storm erosivity using idealized intensity distributions. *Trans. ASAE* 30, 379–386.
- Casson, N.J., Eimers, M.C., Watmough, S.A., 2014. Controls on soil nitrification and stream nitrate export at two forested catchments. *Biogeochemistry* 121, 355–368. <https://doi.org/10.1007/s10533-014-0006-y>.
- Čotar, K., Pehani, P., Veljanovski, T., 2018. Leaf Area Index, MODIS MCD15A3, Obdobje 2002–2016.
- Exner-Kittridge, M., Strauss, P., Blöschl, G., Eder, A., Saracevic, E., Zessner, M., 2016. The seasonal dynamics of the stream sources and input flow paths of water and nitrogen of an Austrian headwater agricultural catchment. *Sci. Total Environ.* 542, 935–945 The Authors.
- Feinson, L.S., Gibb, J., Imbrigiotta, T.E., Garrett, J.D., 2016. Effects of land use and sample location on nitrate-stream flow hysteresis descriptors during storm events. *J. Am. Water Resour. Assoc.* 52 (6), 1493–1508.
- Gundersen, P., Callesen, I., de Vries, W., 1998. Nitrate leaching in forest ecosystems is related to forest floor C/N ratios. *Environ. Pollut.* 102, 403–407.
- Heiser, M., Scheidl, C., Eisl, J., Spangl, B., Hübl, J., 2015. Process type identification in torrential catchments in the eastern Alps. *Geomorphology* 232, 239–247. <https://doi.org/10.1016/j.geomorph.2015.01.007>.
- Huebsch, M., Fenton, O., Horan, B., Hennessy, D., Richards, K.G., Jordan, P., Goldscheider, N., et al., 2014. Mobilisation or dilution? Nitrate response of karst springs to high rainfall events. *Hydrol. Earth Syst. Sci.* 18 (11), 4423–4435.
- Judd, K.E., Likens, G.E., Groffman, P.M., 2007. High nitrate retention during winter in soils of the Hubbard Brook Experimental Forest. *Ecosystems* 10 (2), 217–225.
- Kassambara, A., 2018. Machine Learning Essentials: Practical Guide in R. STHDA.
- Keller, A.A., Fox, J., 2019. Giving credit to reforestation for water quality benefits. *PLoS ONE* 14 (6), 1–18.
- Kobold, M., Sušelj, K., 2004. Padavinske napovedi in njihova nezanesljivost v hidrološkem prognoziraju. *Zbornik: Raziskave s področja geodezije in geofizike 2004*, pp. 61–75.
- Koenig, L.E., Shattuck, M.D., Snyder, L.E., Potter, J.D., McDowell, W.H., 2017. Deconstructing the effects of flow on DOC, nitrate, and major ion interactions using a high-frequency aquatic sensor network. *Water Resour. Res.* 53 (12), 10655–10673.
- Li, G., Wan, L., Cui, M., Wu, B., Zhou, J., 2019. Influence of canopy interception and rainfall kinetic energy on soil erosion under forests. *Forests* 10 (6). <https://doi.org/10.3390/f10060509> available at.
- Lovett, G., Weathers, K., Arthur, M., 2002. Control of nitrogen loss from forested watersheds by soil carbon: nitrogen ratio and tree species composition. *Ecosystems* 5, 0712–0718. <https://doi.org/10.1007/s10021-002-0153-1>.
- Markart, G., Teich, M., Scheidl, C., Kohl, B., 2021. Flood protection by forests in alpine watersheds: lessons learned from Austrian case studies. In: Teich, M., Accastello, C., Perzl, F., Kleemayr, K. (Eds.), *Protective Forests as Ecosystem-based Solution for Disaster Risk Reduction (ECO-DRR)* <https://doi.org/10.5772/intechopen.99507> available at.
- Mikoš, M., Kranjc, A., Matičič, B., Müller, J., Rakovec, J., Roš, M., Brilly, M., 2002. Hidrološko izrazje = Terminology in hydrology. *Acta Hydrotech.* 20, 3–325.
- MKGP, 2018. Grafični podatki RABA za celo Slovenijo = RABA Graphic Data for the Whole Slovenia.
- Mohammad, A.G., Adam, M.A., 2010. The impact of vegetative cover type on runoff and soil erosion under different land uses. *Catena* 81 (2), 97–103 Elsevier B.V.
- Moravcová, J., Pavlíček, T., Ondr, P., Koupilová, M., Kvítek, T., 2013. Comparison of parameters influencing the behavior of concentration of nitrates and phosphates during different extreme rainfall-runoff events in small watersheds. *Hydrol. Earth Syst. Sci. Discuss.* 10 (10), 12105–12151.
- Ogris, N., Kobler, A., Čotar, K., Pehani, P., Veljanovski, T., 2018. VegX – Vegetacijski indeksi v Sloveniji, spletna aplikacija in interaktivna karta. available at: Gozdarski inštitut Slovenije, Znanstvenoraziskovalni center Slovenske akademije znanosti in umetnosti. <https://www.zdravgozd.si/projekti/vegx/>.
- Parra Suárez, S., Peiffer, S., Gebauer, G., 2019. Origin and fate of nitrate runoff in an agricultural catchment: Haeam, South Korea – comparison of two extremely different monsoon seasons. *Sci. Total Environ.* 648, 66–79 Elsevier B.V.
- Pellerin, B.A., Stauffer, B.A., Young, D.A., Sullivan, D.J., Bricker, S.B., Walbridge, M.R., Clyde, G.A., et al., 2016. Emerging tools for continuous nutrient monitoring networks: sensors advancing science and water resources protection. *J. Am. Water Resour. Assoc.* 52 (4), 993–1008.
- R Core Team, 2018. R: a language and environment for statistical computing. available at: R Foundation for Statistical Computing, Vienna, Austria. <https://www.r-project.org>.
- Ross, C.A., Casson, N.J., Tenuwara, M., 2021. Linking dominant rainfall-runoff event hydrologic response dynamics with nitrate and chloride load estimates of three boreal shield catchments. *J. Geophys. Res. Biogeosci.* 126 (9), 1–14.
- Roth, B.E., Slatton, K.C., Cohen, M.J., 2007. On the potential for high-resolution lidar to improve rainfall interception estimates in forest ecosystems. *Front. Ecol. Environ.* 5 (8), 421–428.
- Rusjan, S., Mikoš, M., 2008. Assessment of hydrological and seasonal controls over the nitrate flushing from a forested watershed using a data mining technique. *Hydrol. Earth Syst. Sci.* 12 (2), 645–656.
- Rusjan, S., Vidmar, A., 2017. The role of seasonal and hydrological conditions in regulating dissolved inorganic nitrogen budgets in a forested catchment in SW Slovenia. *Sci. Total Environ.* 575, 1109–1118 Elsevier B.V.
- Sapač, K., Bezák, N., Vidmar, A., Rusjan, S., 2021. Nitrate nitrogen (NO₃-N) export regimes based on high-frequency measurements in the Kuzlovec stream catchment. *Acta Hydrotech.* 34 (60), 25–38.
- Sapač, K., Vidmar, A., Bezák, N., Rusjan, S., 2020. Lag times as indicators of hydrological mechanisms responsible for NO₃-N flushing in a forested headwater catchment. *Water* 12 (3), 1092.
- Schlesinger, W.H., Jasechko, S., 2014. Transpiration in the global water cycle. *Agric. For. Meteorol.* 189–190, 115–117 Elsevier B.V.
- Sebestyen, S.D., Shanley, J.B., Boyer, E.W., Kendall, C., Doctor, D.H., 2014. Coupled hydrological and biogeochemical processes controlling variability of nitrogen species in streamflow during autumn in an upland forest. *Water Resour. Res.* 50 (2), 1569–1591.
- Snyder, L., Potter, J.D., McDowell, W.H., 2018. An evaluation of nitrate, fDOM, and turbidity sensors in New Hampshire streams. *Water Resour. Res.* 54 (3), 2466–2479.
- Teng, M., Huang, C., Wang, P., Zeng, L., Zhou, Z., Xiao, W., Huang, Z., et al., 2019. Impacts of forest restoration on soil erosion in the Three Gorges Reservoir area, China. *Sci. Total Environ.* 697 (1), 134164 Elsevier B.V.
- Winter, C., Nguyen, T.V., Musolff, A., Lutz, S.R., Rode, M., Kumar, R., Fleckenstein, J.H., 2022a. Droughts Can Reduce the Nitrogen Retention Capacity of Catchments. *EGU*sphere, pp. 1–25 Preprint, No. June.
- Winter, C., Tarasova, L., Lutz, S.R., Musolff, A., Kumar, R., Fleckenstein, J.H., 2022b. Explaining the variability in high-frequency nitrate export patterns using long-term hydrological event classification. *Water Resour. Res.* 58 (1). <https://doi.org/10.1029/2021WR030938> available at.
- Yang, J., Heidbüchel, I., Musolff, A., Reinstorf, F., Fleckenstein, J.H., 2018. Exploring the dynamics of transit times and subsurface mixing in a small agricultural catchment. *Water Resour. Res.* 54 (3), 2317–2335.
- Yao, Y., Dai, Q., Gao, R., Gan, Y., Yi, X., 2021. Effects of rainfall intensity on runoff and nutrient loss of gently sloping farmland in a karst area of SW China. *PLoS ONE* 16 (3 March), 1–18.
- Zabret, K., Šraj, M., 2015. Can urban trees reduce the impact of climate change on storm runoff? *Urbani Izziv* 26 (2014), 165–178.
- Zhang, D., Wang, Z., Guo, Q., Lian, J., Chen, L., 2019. Increase and Spatial Variation in Soil Infiltration Rates Associated With Fibrous and Tap Tree Roots, pp. 1–12.
- Zhang, X., Friedl, M.A., Schaaf, C.B., Strahler, A.H., Hodges, J.C.F., Gao, F., Reed, B.C., et al., 2003. Monitoring vegetation phenology using MODIS. *Remote Sens. Environ.* 84 (3), 471–475.